A Molecular Magnet Confined in the Nanocage of a Globular Protein

Rajib K. Mitra,[a] Pramod K. Verma,[a] Dirk Wulferding,[b] Dirk Menzel,[b] Tamoghna Mitra,[c] Ana M. Todea,[c] Peter Lemmens,*[b] Achim Müller,[c] and Samir K. Pal*[a]

Dedicated to Prof. Rüdiger Kniep on the occasion of his 65th birthday

The effect of confinement and energy transfer on the dynamics of a molecular magnet, known as a model system to study quantum coherence, is investigated. For this purpose the well-known polyoxovanadate $[V_{15}As_6O_{42}(H_2O)]^{6-}$ (V_{15}) is incorporated into a protein (human serum albumin, HSA) cavity. Due to a huge overlap of the optical absorption spectrum of V_{15} with the emission spectrum of a fluorescence center of HSA (con-taining a single tryptophan residue), energy transfer is induced and probed by steady-state and time-resolved fluorescence. The geometrical coordination and the distance of the confined V_{15} to the tryptophan moiety of HSA are investigated at vari-ous temperatures. This effect is used as a local probe for the thermal denaturation of the protein at elevated temperatures.

1. Introduction

Recently a new class of magnetic materials, called molecular magnets, has attracted much attention due to their unusual properties that in general are associated with mesoscopic magnetism and quantum effects.[1,2] These materials allow the study of spin relaxation in nanomagnets, quantum tunneling of magnetization, topological quantum phase interference, and quantum coherence.[3,4] Among these materials, the poly-oxovanadate $[V_{15}As_6O_{42}(H_2O)]^{6-}$ cluster (hereafter denoted as V_{15}) possesses a triple-layered structure of 15 antiferromagneti-cally coupled V^{IV} ions.[5-7] In contrast to molecular magnets (e.g., Mn_{12} or Fe_8), the antiferromagnetic interactions of V_{15} lead to only a small uncompensated total spin of $S = \frac{1}{2}$ with very weak anisotropy.[8-12] The energy pattern of V_{15} contains two low-lying levels well separated from the excited ones. V_{15} shows the essential properties of a single-molecule magnet: a tunneling splitting of low-lying spin states leading to a pro-nounced magnetic hysteresis. Furthermore, the observation of Rabi quantum oscillations in a sample of diluted molecules demonstrates that the quantum coherence[9,13] of the spin tun-neling processes can be preserved to some extent.[14] Our inter-est is to search for and control the decoherence mechanisms and related energy transfer in quantum systems with electro-magnetic fields applied in the visible range, that is, at higher energies than ESR or NMR experiments.[14] The dipolar, excited-state interactions involved are different from interactions via the spin bath that are usually discussed.[9]

Herein, we report primary observations of the spectroscopic and magnetic properties of V_{15} upon its incorporation into the cavity of a well-known protein. We achieved three goals: the confinement protects the V_{15} clusters from aggregation, it sta-bilizes the clusters, and it allows the study of energy transfer and the optical dynamics by using fluorescence spectroscopy. The latter effect is possible due to the cluster's proximity to a fluorescence center in the protein. The strong distance de-pendence of the energy transfer allows the molecular magnet to be used for the first time as a molecular ruler and the ge-ometry of a protein to be probed with nanometer resolution. As a case study, we demonstrate the effect of temperature-in-duced denaturation on the fluorescence dynamics.

Experimental Section

The molecular magnet V_{15} was prepared as previously described.[5] The globular transport protein human serum albumin (HSA) of size 66 kDa was of the highest available purity (99%) and was obtained from Sigma. The HSA–V_{15} conjugate was prepared by mixing the requisite volume of 25 μM HSA solution and V_{15} solution followed by prolonged stirring to ensure complete complexation. The rela-tive concentration ratio in the final HSA–V_{15} solution was main-tained at HSA/V_{15} = 2:1. Complete complexation of V_{15} with HSA was confirmed from the stability of the V_{15} clusters in the solution. As shown in Figure 1a, the absorption spectrum of V_{15} in water changes substantially with time. Please note that we used a very dilute aqueous solution of V_{15} without degassing it. The reaction with O_2 is a very probable candidate for a decomposition reaction related to the observed significant decrease of the optical density

[a] Dr. R. K. Mitra, P. K. Verma, Dr. S. K. Pal
Unit for Nano Science and Technology
Department for Chemical, Biological and Macromolecular Sciences
S.N. Bose National Centre for Basic Sciences
Block JD, Sector III, Salt Lake, Kolkata 700098 (India)
E-mail: skpal@bose.res.in
p.lemmens@tu-bs.de

[b] D. Wulferding, Dr. D. Menzel, Prof. Dr. P. Lemmens
Institute for Condensed Matter Physics, TU Braunschweig
Mendelssohnstr. 3, 38106 Braunschweig (Germany)

[c] Dr. T. Mitra, Dr. A. M. Todea, Prof. Dr. A. Müller
Fakultät für Chemie, Universität Bielefeld
Postfach 100131, 33501 Bielefeld (Germany)

Supporting information for this article is available on the WWW under http://dx.doi.org/10.1002/cphc.200900708.

(OD) at 350 nm.[15–17] The time-dependent change of absorption at 350 nm (Figure 1 b) shows that the OD of V_{15} clusters in the protein solution is invariant. The enhanced stability of the V_{15} clusters
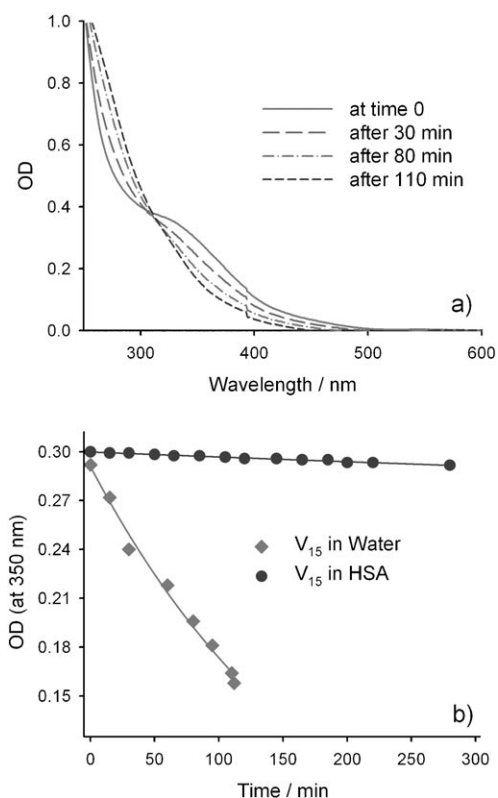

Figure 1. a) Absorption spectra of a very dilute solution of V_{15} in undegassed water at different time intervals. b) Time-dependent absorption profiles of V_{15} at 350 nm in water and HSA. From the kinetics an enhanced stability of V_{15}, especially against oxidation in HSA, is evident.

clearly indicates the complexation of the clusters with the protein, which in turn protects V_{15} against oxidation by oxygen and also justifies the integrity of the sample solution within our experimental time span.

Steady-state absorption and emission were measured with a Shimadzu UV-2450 spectrophotometer and Jobin Yvon Fluoromax-3 fluorimeter, respectively. Fluorescence transients were measured and fitted by using a commercially available spectrophotometer (LifeSpec-ps, Edinburgh Instruments, UK) with an 80 ps instrument response function (IRF) and an attachment for temperature-dependent studies (Julabo, Model F32). The details of the time-resolved measurements are given in the Supporting Information. The circular dichroism (CD) and fluorescence-detected circular dichroism (FDCD) spectra were measured in a Jasco 815 spectrometer with a Peltier setup for the temperature-dependent measurements.

Magnetic susceptibility measurements were performed using a superconducting quantum interference device (SQUID) magnetometer (Quantum Design) as a function of temperature (2–250 K) and magnetic field (0.1, 1, and 7 T). Due to the small magnetic moment of each molecular magnet ($S=\frac{1}{2}$), the restricted sample volume, and the small mass of the V_{15} clusters (ratio of molar masses m_{HSA}:$m_{V_{15}}=30$), we used only the low-temperature limit (up to 6 K) of the data for a comparison with the susceptibility of bulk crystals

of V_{15} (sample weight 65×10^{-3} g). In separate steps we measured the susceptibility of the bulk V_{15} reference sample of the molecular magnet, $\chi_{V_{15}}$, which shows good agreement with the literature,[1] a sample (sample weight $m_{total}=3.6\times10^{-3}$ g) of the diluted molecular magnets in confinement, χ_{total}, and a similar amount of the protein without doping, χ_{HSA}, which also served as an approximation for the diamagnetic contribution of the sample holder. Figure 2 shows the inverse of the difference $\chi^{-1}=\alpha(\chi_{total}-\chi_{HSA})^{-1}$ multiplied with a reference factor α to match to bulk V_{15}. Within our accuracy the bulk and diluted V_{15} show the same temperature dependence. The scaling parameter $\alpha=\frac{1}{5}$ corresponds to one V_{15} cluster per five HSA proteins.[14] This order of magnitude agreement is acceptable when taking into account the small sample weight of doped HSA. Note that at low temperatures one can expect magnetically anisotropic contributions arising from the antisymmetric exchange, which are important for the energy pattern of the low-lying levels of V_{15}.[18,19] This indeed leads to a deviation from the Curie law at low temperatures.
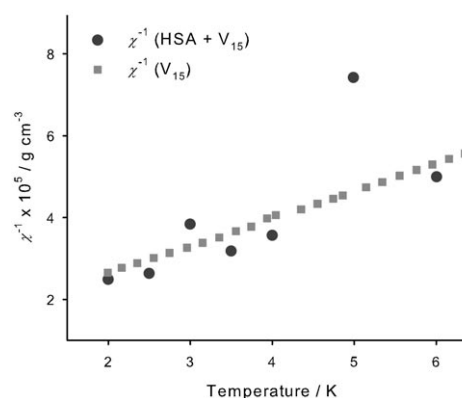

Figure 2. Inverse magnetic susceptibility $\chi^{-1}=\alpha(\chi_{total}-\chi_{HSA})^{-1}$ of V_{15} in HSA with the diamagnetic contribution of the sample holder and HSA subtracted and a fitting parameter $\alpha=\frac{1}{5}$. The data are matched to the inverse susceptibility of bulk V_{15}. The experiments are performed in a magnetic field of 0.1 T.

2. Results and Discussion

The absorption spectrum of an aqueous solution of V_{15} is found to be rather featureless within the experimental window, only producing a shoulder around the 330 nm region (Figure 3 a). The emission spectrum of V_{15} (excited at 330 nm) in aqueous solution also does not show any characteristic feature (not exemplified), thus indicating the lack of any excited-state phenomenon associated with the cluster. On the other hand, the absorption spectrum of HSA produces a peak at 280 nm, which is attributed to the presence of the single tryptophan residue (Trp214; not shown). We excited HSA at 300 nm to avoid emission from the other possible fluorophores, such as tyrosine or phenylalanine, present in the protein. The fluorescence spectrum of HSA in water produces a single peak at ≈350 nm (Figure 3 a). A small hump is also observed in the 335 nm region of the spectrum, which is the Raman signal of water arising from the 300 nm excitation. With an increase in temperature from 293 to 333 K, the fluorescence intensity of HSA is quenched appreciably (Figure 3 b). This
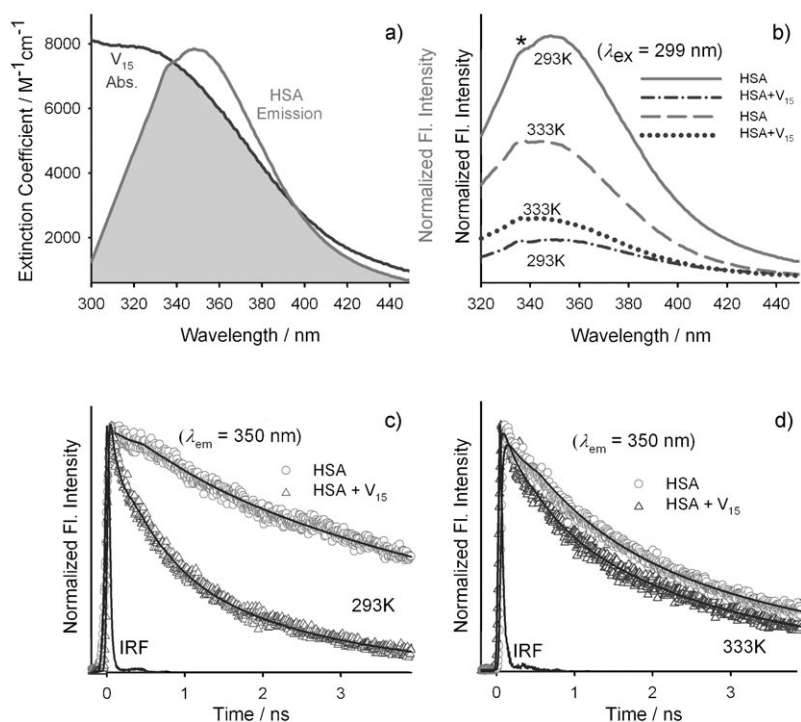
Figure 3. a) Absorption and emission spectra of V_{15} and HSA in aqueous solution. The shaded region is the area of overlap between the two spectra. This area is a measure of the distance between the donor (Trp residue of HSA) and V_{15} (see text for details). b) Effect of temperature on the emission spectrum of HSA in the absence and presence of V_{15}; (*) represents a Raman signal. c,d) Time-resolved fluorescence decay of the Trp residue in HSA measured at 350 nm in the absence and presence of V_{15} at 293 (c) and 333 K (d). The solid lines are bi (or tri)-exponential decay fitted curves.

(64%), 440 (18%), and 2090 ps (18%), with the average lifetime of the HSA–V_{15} conjugate $<\tau_{DA}> = 470$ ps. This indicates a quenching of fluorescence by more than an order of magnitude. As the temperature is increased, $<\tau_D>$ of HSA decreases steadily and at 333 K it becomes half of the value at 293 K (Table 1). However, in the presence of V_{15}, $<\tau_{DA}>$ steadily increases, leading to a value five times larger at 333 K than that at 293 K (Table 1). Such a reversal of the temperature effect is quite unusual. We attribute the fast component (of the order of tens of picoseconds), which is present in the conjugate and absent in HSA, to the quenching of the fluorophore upon addition of V_{15}. With an increase in temperature this component becomes gradually slower and signifies the release of quenching, similar to the steady-state measurements (Figure 3 b).

In the following we discuss the origin of the quenching in the V_{15}–HSA conjugate. To distinguish a trivial, structural, or defect origin from an intrinsic electronic effect, the structural

quenching is related to a denaturation and unfolding of the compact globular protein in which the Trp214 is exposed to the aqueous environment, thus decreasing its fluorescence intensity.[20, 21]

The emission of HSA suffers a huge quenching upon complexation with V_{15} (Figure 3 b). We highlight the fact that the origins of the temperature-induced and V_{15}-induced quenching are rather different. To gain a better insight into the observed quenching, time-resolved fluorescence measurements of the systems were performed (Figures 3 c,d and Table 1). The decay transient of HSA at 293 K can be fitted biexponentially with time constants of 880 (15%) and 5850 ps (85%), with an average lifetime ($<\tau_D>$) of 5090 ps (Table 1). In the presence of V_{15} the decay is dominated by a fast component and could only be fitted triexponentially with time constants of 20

Table 1. Time-resolved fluorescence decay and FRET data of the Trp214 residue in HSA at different temperatures in the absence and presence of V_{15}. Values in parentheses represent the relative weight of the time component.

	T [K]	τ_1 [ps]	τ_2 [ps]]	τ_3 [ps]	$<\tau_D>$ [ps]	$<\tau_{DA}>$ [ps]	E	$J(\lambda)$ $\times 10^{13}$	R [Å]
HSA in water	293	880 (0.15)	5850 (0.85)	–	5090	–	–	–	–
	303	1370 (0.30)	5850 (0.70)	–	4500	–	–	–	–
	313	830 (0.26)	4900 (0.74)	–	3820	–	–	–	–
	323	800 (0.30)	4350 (0.70)	–	3280	–	–	–	–
	333	1030 (0.42)	4050 (0.58)	–	2780	–	–	–	–
HSA + V_{15}	293	20 (0.64)	440 (0.18)	2090 (0.18)	–	470	0.91	9.03	16.0
	303	50 (0.51)	790 (0.29)	2280 (0.20)	–	710	0.84	9.00	17.5
	313	80 (0.44)	1030 (0.41)	3270 (0.15)	–	950	0.75	9.00	19.0
	323	100 (0.42)	1040 (0.37)	4020 (0.21)	–	1290	0.60	8.97	21.5
	333	340 (0.29)	1500 (0.37)	4170 (0.34)	–	2070	0.25	8.97	28.0

integrity of both the protein and the molecular magnet has to be assured. The CD spectrum of the protein was measured in the presence and absence of the molecular magnet, and it was found that the CD spectrum of HSA does not alter when V_{15} is confined (data not shown). This indicates that incorporation of V_{15} in HSA does not perturb its tertiary structure. In addition, the above-described absorption studies (Figure 1) demonstrate the enhanced stability of V_{15} in confinement. Therefore, we take an electronic effect into consideration.

With the given geometry and distances in the nanometer range the effect of mediated exchange or excited-state hopping processes should be negligible. However, energy transfer by radiationless dipole–dipole coupling is an efficient way to modify the electronic dynamics of a molecular system. This process, related to the Förster resonance energy transfer (FRET), is based on a spectral overlap between the excited-state dipole (donor) of the Trp in HSA with a dipole (acceptor) in the molecular magnet. Figure 3a does indeed reveal a huge overlap of the emission spectrum of HSA with the absorption spectrum of V_{15}. The resulting energy transfer leads to an efficient modification of the fluorescence dynamics of the Trp in HSA, and therefore an efficient quenching of its emission spectrum can be expected.

Previous experimental and theoretical studies of molecular magnetism and their environmental spin decoherence were related to the effect of spin–phonon and spin–orbit interactions to an external bath. Both interactions are reduced for small spin systems and it has been claimed that the Rabi oscillations on a 10^{-6} s timescale, due to coupling to a coherent electromagnetic field, are possible because of the sufficient suppression of further dipolar couplings.[14] The present investigations show that there are excited-state dipolar couplings relevant on a much faster (100 ps) timescale and higher (2 eV) energy scale. Nevertheless, the related decoherence might be relevant in all cases in which optical schemes are involved, either for the manipulation/readout operations or other handlings of the molecular species.

In the following we use the well-known thermal denaturation of the confining protein to further elucidate the potential of the observed energy transfer between the molecular magnet and the protein. This is an initial melting of the globule state that leads to an irreversible unfolding of the protein for temperatures higher than 328 K.[20–22]

In the temperature range from 293 to 333 K the CD spectrum of HSA suffers only a moderate effect, but when the temperature is increased to 343 K considerable change is produced (Figure 4). Specific changes occurring at the fluorophore-containing region of the protein can be probed by specific FDCD spectra of the protein. Also in FDCD (see inset of Figure 4), only moderate changes occur up to 333 K followed by a considerable change at 343 K. The extent of the changes resembles those of the CD spectra, which confirms that the thermal unfolding does affect the Trp-containing domain of HSA, and ensures that the FRET at different temperatures provides information on the unfolding pathway of the protein.

From the average lifetime $<\tau_D>$ of the donor (HSA), $<\tau_{DA}>$ of the conjugate (HSA + V_{15}), and the extent of the overlap between the emission spectrum of HSA and the absorption spectrum of V_{15}, the distance between Trp and V_{15} can be determined following the details given in the Supporting Information. The distances calculated at different tempera-
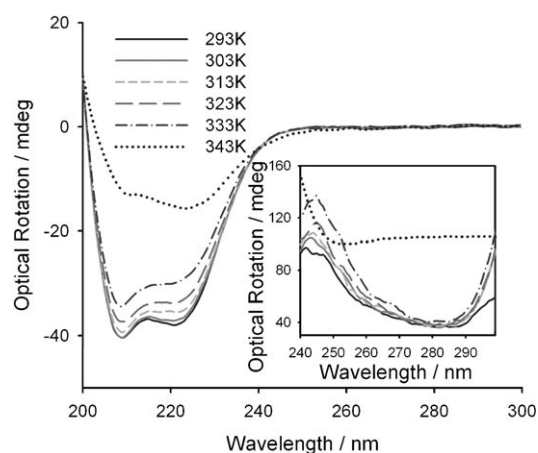

Figure 4. CD spectra of HSA at different temperatures. Inset: the corresponding FDCD spectra.

tures (Table 1) are well within the range of the interdomain distance of the protein.[23] This further supports the interaction between the entrapped V_{15} and Trp.[22] With an increase in temperature, the donor–acceptor distance (R) increases first gradually and then rapidly as the temperature crosses 330 K (Figure 5), which is very much consistent with the irreversible thermal denaturation of the protein. The increase in R indicates a temperature-induced interdomain separation of the protein, as evidenced earlier by the increase in the size of the protein measured by the dynamic light scattering (DLS) technique.[21, 22] In this way, V_{15} is applied as a molecular marker for the protein folding process.

All relative changes in CD, FDCD, energy-transfer efficiency E, and R are plotted as a function of temperature in Figure 6 to summarize the results. Two characteristic regimes are evident and marked in different shades with a discontinuity at ≈330 K. The values for E, R, and FDCD are quite comparable, whereas those for CD are smaller. The measurements of E and R correspond to the fluorescence signals of Trp, which in turn are associated with the FDCD signals, whereas the CD signals give an overall view of the changes in the tertiary structure of the protein. The comparability of the R and FDCD values indicates that the resonance energy transfer of Trp with V_{15} is a perfect tool to extract information on the changes in the structure of the protein, especially of the Trp-containing domain.

3. Conclusions

In summary, the complexation and confinement of V_{15} in the globular protein HSA leads to an enhanced stability without perturbing its magnetic properties or the tertiary structure of the protein. Resonance energy transfer via excited-state dipole–dipole interaction is probed by steady-state and time-resolved fluorescence spectroscopy of the confining HSA. The
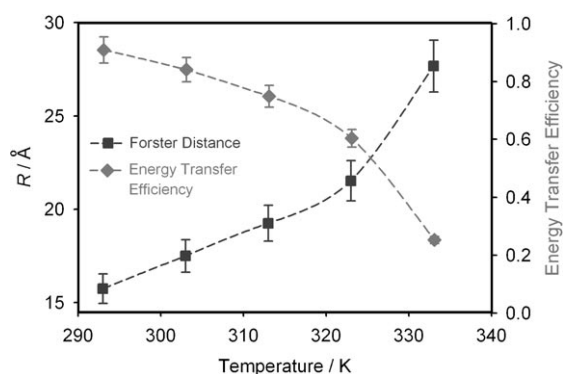
Figure 5. Energy-transfer efficiency (*E*) and donor–acceptor distance (*R*) measured from HSA–V$_{15}$ energy-transfer processes at different temperatures. The dotted lines are guides to the eye.
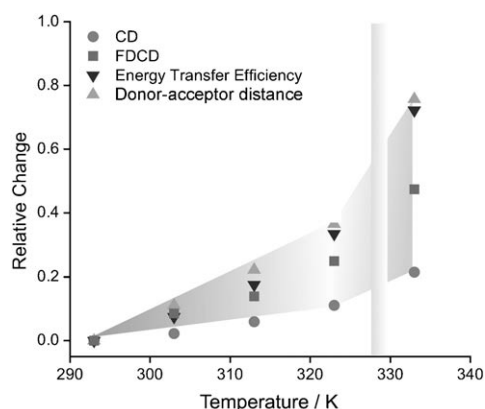

Figure 6. Relative change of CD, FDCD, energy-transfer efficiency (*E*), and donor–acceptor distance (*R*) as a function of temperature. The gray region at 330 K indicates the onset temperature of the irreversible unfolding process of HSA.

consistent temperature dependencies and absolute magnitude of molecular distances and other parameters sampled during a denaturation study of the protein support the FRET calculation scheme. We also propose that the overlap between the emission and absorption spectra is an important parameter for the spin decoherence of the conjugates if optical schemes for manipulation or readout of the molecular magnets are involved.

Acknowledgements

[1] D. Gatteschi, A. Caneschi, L. Pardi, R. Sessoli, *Science* **1994**, *265*, 1054–1058.
[2] O. Kahn, *Molecular Magnetism*, VCH, New York, **1993**.
[3] J. R. Friedman, M. P. Sarachik, J. J. Tejada, R. R. Ziolo, *Phys. Rev. Lett.* **1996**, *76*, 3830–3833.
[4] L. Thomas, F. Lionti, R. Ballou, D. Gatteschi, R. Sessoli, B. Barbara, *Nature* **1996**, *383*, 145–147.
[5] A. Müller, J. Döring, *Angew. Chem.* **1988**, *100*, 1789; *Angew. Chem. Int. Ed. Engl.* **1988**, *27*, 1721.
[6] D. Gatteschi, L. Pardi, A. L. Barra, A. Müller, J. Döring, *Nature* **1991**, *354*, 463–465.
[7] A. L. Barra, D. Gatteschi, L. Pardi, A. Mueller, J. Doering, *J. Am. Chem. Soc.* **1992**, *114*, 8509–8514.
[8] I. Chiorescu, W. Wernsdorfer, A. Müller, H. Bögge, B. Barbara, *Phys. Rev. Lett.* **2000**, *84*, 3454–3457.
[9] V. V. Dobrovitski, M. I. Katsnelson, B. N. Harmon, *Phys. Rev. Lett.* **2000**, *84*, 3458–3461.
[10] G. Chaboussant, R. Basler, A. Sieber, S. T. Ochsenbein, A. Desmedt, R. E. Lechner, M. T. F. Telling, P. Kögerler, A. Müller, H.-U. Güdel, *Europhys. Lett.* **2002**, *59*, 291–297.
[11] D. Procissi, B. J. Suh, J. K. Jung, P. Kögerler, R. Vincent, F. Borsa, *J. Appl. Phys.* **2003**, *93*, 7810–7812.
[12] I. Rudra, S. Ramasesha, D. Sen, *J. Phys. Condens. Matter* **2001**, *13*, 11717–11725.
[13] B. E. Kane, *Nature* **1998**, *393*, 133–138.
[14] S. Bertaina, S. Gambarelli, T. Mitra, B. Tsukerblat, A. Müller, B. Barbara, *Nature* **2008**, *453*, 203–206.
[15] The related solid compound (complete formula K$_6$[V$_{15}$As$_6$O$_{42}$(H$_2$O)]·8H$_2$O) shows bands according to electronic transitions at 365, 540 (sh), and 800 nm.[16] The band positions are practically identical to those in aqueous solution, whereas the characteristic d–d bands at approximately 540 (sh) and 800 nm (in contrast to the UV band) can only be observed at higher concentrations and correspond to the expected ones.[17] In the thesis of Döring,[16] the characteristic Raman bands (1000 (vs), 976 (w), 949 (m), 861 (m), 792 (m), and 416 (m) cm^{-1}; excitation line 514.5 nm) are also given, which allow the identification of V$_{15}$ in solution. The preparation of the compound is performed at a pH value of ≈6.8, while the pH value of a solution of concentration 2 mg mL^{-1} is ≈5.3. It should be realized that the cluster is oxygen sensitive, which especially plays a role in dilute solutions if the solvent is not degassed, as in the present investigation. This was the case in ref. [14] where the cluster was also additionally protected against oxidation by its extraction after encapsulation.
[16] J. Döring, PhD thesis, University of Bielefeld, **1990**.
[17] A. B. P. Lever, *Inorganic Electronic Spectroscopy*, Elsevier, Amsterdam, **1984**.
[18] B. Tsukerblat, A. Tarantul, A. Müller, *J. Mol. Struct.* **2007**, *838*, 124–132.
[19] A. Tarantul, B. Tsukerblat, A. Müller, *Inorg. Chem.* **2007**, *46*, 161–169.
[20] K. Flora, J. D. Brennan, G. A. Baker, M. A. Doody, F. V. Bright, *Biophys. J.* **1998**, *75*, 1084–1096.
[21] R. K. Mitra, S. S. Sinha, S. K. Pal, *Langmuir* **2007**, *23*, 10224–10229.
[22] S. S. Sinha, R. K. Mitra, S. K. Pal, *J. Phys. Chem. B* **2008**, *112*, 4884–4891.
[23] S. Sugio, A. Kashima, S. Moshizuki, M. Noda, K. Kobayashi, *Protein Eng.* **1999**, *12*, 439–446.